

Greener waterborne epoxy coatings with optimized UV-resistance

Mauro Sergio da Silva¹ , Alana Gabrieli de Souza² , Derval dos Santos Rosa^{2*} ,
Ticiane Sanches Valera¹  and Hélio Wiebeck¹ 

¹*Departamento de Engenharia Metalúrgica e de Materiais – PMT, Escola Politécnica – POLI, Universidade de São Paulo – USP, São Paulo, SP, Brasil*

²*Centro de Engenharia, Modelagem, e Ciências Sociais Aplicadas – CECS, Universidade Federal do ABC – UFABC, Santo André, SP, Brasil*

*derval.rosa@ufabc.edu.br

Abstract

The UV-resistance performance of waterborne epoxy coatings with different aminic-curable substances was evaluated to solve the widely known problem of poor weathering resistance of coatings. Samples were evaluated by color and gloss changes, FTIR, thermal properties, and macroscopic morphology. Results indicated that higher aminic values in curing agents degraded faster than lower aminic values (increases of ~3% in delta b and delta E between 5 and 20%). All samples showed a gloss variation varying between 40 and 70 G.U. FTIR and Tg indicated the resin degradation when using curing agents of unmodified aliphatic amine because of its rapid chemical degradation under a UV environment, as confirmed by microscopy images. The curing agents with aminic values between 200 and 300 KOH/g and the equivalent weight of amine hydrogen higher than 120 g/eq showed the best performance in epoxy coatings and good stability against accelerated aging, being promising options for future applications.

Keywords: epoxy coatings, curing agent, yellowing, weathering.

How to cite: Silva, M. S., Souza, A. G., Rosa, D. S., Valera, T. S., & Wiebeck, H. (2024). Greener waterborne epoxy coatings with optimized UV-resistance. *Polímeros: Ciência e Tecnologia*, 34(3), e20240034. <https://doi.org/10.1590/0104-1428.20230133>.

1. Introduction

Epoxy resins play an important role as protective coatings due to their chemical inertness that allows good corrosion protection, besides their chemical resistance, electrical insulation properties, and adhesion to heterogeneous substrates. Two-component epoxy/amine systems are widely used in civil construction and industrial maintenance. However, the currently used systems generally contain high levels of volatile organic compounds (VOCs) that are harmful to human health and the environment. Thus, to improve the environmentally friendly character of this class of materials, there is a movement to shift the solvent-borne system to waterborne ones^[1]. As an example, the European Union in the Directive 2004/42/CE of the European Parliament and of the Council of 21 April 2004 stated the maximum rates of volatile organic compounds for several types of coatings.

Waterborne coatings are widely used as an effective method of protecting against corrosion on metallic substrates, and several works have reported the importance and effectiveness of these materials. Wang et al. (2019)^[1] prepared waterborne epoxy coatings with graphene modified with lignin for anticorrosive applications and reported that nanocomposite coatings showed an anti-corrosion effect due to the labyrinth effect caused by the fillers. Sheng et al.^[2] prepared waterborne polyurethane composites containing

MXene nanosheets and reported low corrosion current and UV-blocking properties.

Despite the excellent applicability and economic interest, epoxy systems are sensitive to exposure to UV radiation, not only as a function of the incidence of sunlight but also of the visible light spectrum^[3]. The polymeric structure undergoes photochemical damage on the surface of the applied paint film, resulting in its degradation^[4]. The use of additives that block and absorb UV radiation is common to delay this effect but results in high costs and relatively low effectiveness for long periods of exposure during the working time of the painted substrate^[2,5]. As a result of the degradation process, the coatings are subjected to chalking, gloss loss, and yellowing, decreasing the coating capacity to shield the substrate, and implying a complete loss of function^[6,7]. Liu et al.^[8] prepared waterborne epoxy resin containing emulsified asphalt to improve mechanical properties and reported waterproof performance, aging, and wear resistance. Li et al.^[7] prepared epoxy coating with polyetheramine-functionalized graphene oxide and reported that the filler was important to avoid the yellowing of the coating, quantified by color parameters.

Substantial work has been done to improve the weathering resistance of waterborne epoxy coatings to guarantee long

shelf-life for these materials without property loss, such as color, mechanical resistance, and others^[9-12]. Among the main properties, several additives are usually incorporated, such as nanoparticles, graphene, etc. However, even with a wide range of possibilities, there is still a knowledge gap in efficient additives that delay or prevent the degradation of epoxy coatings during application, which is a technical-scientific challenge. Aiming to expand the possibilities of use and application materials, this work proposes the development of waterborne epoxy coatings using aminicurable substances available on the market to reduce color deterioration and property loss, ensuring good properties for coatings performance.

2. Materials and Methods

2.1 Materials

Westlake Epoxy (Texas, USA) kindly donated the water-based epoxy resin dispersion and the five different types of curing agents (Table 1). The EPI-REZ Resin 7521-WH-57 (resin) has solids of 55-59%, equivalent epoxy weight of 480-600 g/eq, and viscosity at 25 °C of 600-6000 cP. Momentive Performance Materials (New York, USA) donated the leveling additive and the deionized water, and the co-solvent was acquired by The Dow Chemical Company (Michigan, USA). The chemical structures of the curing agents are confidential. Table S1 – Supplementary

Material shows the main properties of all the catalysts. CU abbreviation refers to curing agent.

2.2 Formulation development

The formulations were done based on the stoichiometry of the system considering the ammine hydrogen proportion related to the epoxy content. Usually, the stoichiometry ratio is 1:1 to maximize the crosslinking density, as reported in previous works^[11,12], and it is calculated according to Equation 1, where EW_a is the equivalent weight of ammine and EW_e is the epoxydic equivalent weight, and PHR is the per hundred resin based on the solids.

$$PHR = \frac{EW_a}{EW_e} \times 100 \quad (1)$$

The result represents the amount of curing agent necessary to react with 100 g of epoxydic resin for the proportion 1:1^[13,14].

After initial tests to adjust the raw materials quantities (water, additive, and solvent), 12 formulations were designed to evaluate the curing agent efficiency. The preparation process was divided into two parts: 1—resin preparation and 2—curing agent addition. Before the mixture of parts 1 and 2, the raw materials were weighted separately, according to Table 2.

Table 1. Raw materials used in this work.

Raw material	Description	Characteristics
EPI-REZ Resin 7521-WH-57 (Resin)	Waterborne dispersion of epoxydic resin	Film-forming agent
EPIKURE 8530-W-75	Amine curing agent	Reaction catalyst for epoxy systems
EPIKURE 6870-W-53	Amine curing agent	Reaction catalyst for epoxy systems
EPIKURE 3223	Amine curing agent	Reaction catalyst for epoxy systems
EPIKURE 3234	Amine curing agent	Reaction catalyst for epoxy systems
EPIKURE 8546-W-55	Amine curing agent	Reaction catalyst for epoxy systems
Dowanol DPnB (co-solvent)	Glycol-based solvent	Diluent for waterborne systems
Deionized water (Water)	Waterborne solvent	Diluent for waterborne systems
COATOSIL 28161 (Additive)	Silicon-based additive	Additive to improve paint spread

Table 2. Developed formulations aiming to determine the best proportion between resin and curing agent for the development of waterborne epoxy coatings.

Experiment	Part A - Resin		Part B - Curing agent					Co-solvent	Water
	Resin	Additive	CU-1	CU-2	CU-3	CU-4	CU-5		
1	99.5	0.5	24.5					9.8	14.7
2	99.55	0.45	24.5					9.8	14.7
3	99.5	0.5		47				18.8	28.2
4	99.55	0.45		47				18.8	28.2
5	99.5	0.5					46	18.4	27.6
6	99.55	0.45					46	18.4	27.6
7	99.5	0.5	12.2		2.15			5.74	8.61
8	99.55	0.45	12.2		2.15			5.74	8.61
9	99.5	0.5	12.2				2.5	5.88	8.82
10	99.55	0.45	12.2				2.5	5.88	8.82
11	99.5	0.5	12.3					22.9	7.04
12	99.55	0.45	12.3					22.9	7.04

After the weighting, the parts A and B were mixed following the system stoichiometry for ten minutes and sprayed into rectangular panels using a spray gun HVLP – High Volume Low Pressure, and then left in a chamber free of light, at 25 °C, for seven days, for complete coatings curing, as schematically illustrated in Figure 1.

After the samples had completely cured, accelerated weathering tests were conducted in a QUV-A chamber (Adexim-Comexim, São Paulo, Brazil) with 500 hours of exposure, following the ASTM G154-23^[15]. Throughout the exposure time, the samples were evaluated seven times: 39, 109, 162, 207, 375, 439, and 500 hours.

2.3 Characterization

2.3.1 Appearance changes

The differences in the samples' appearance were quantified by color and gloss measurements. The color was

spectrophotometrically measured in the CIELAB space, in triplicate, similar to the Yari and Rostami work^[16], using a Spectro 2 Guide spectrophotometer (BYK Gardner, Wesel, Germany). The gloss values were measured using a Micro-TRI-Gloss glossmeter (BYK Gardner, Wesel, Germany).

2.3.2 Fourier-transform infrared spectroscopy

FTIR spectra of coatings before and after the weathering were recorded in Spectrum 2 Equipment (PerkinElmer, Connecticut, USA), equipped with an attenuated total reflectance (ATR) accessory. Data acquisition was performed in a range of 500–4000 cm^{-1} , 62 scans, and a spectral resolution of 4 cm^{-1} .

2.3.3 Differential scanning calorimetry

The glass transition temperature (T_g) was analyzed by differential scanning calorimetry (DSC) using a TA

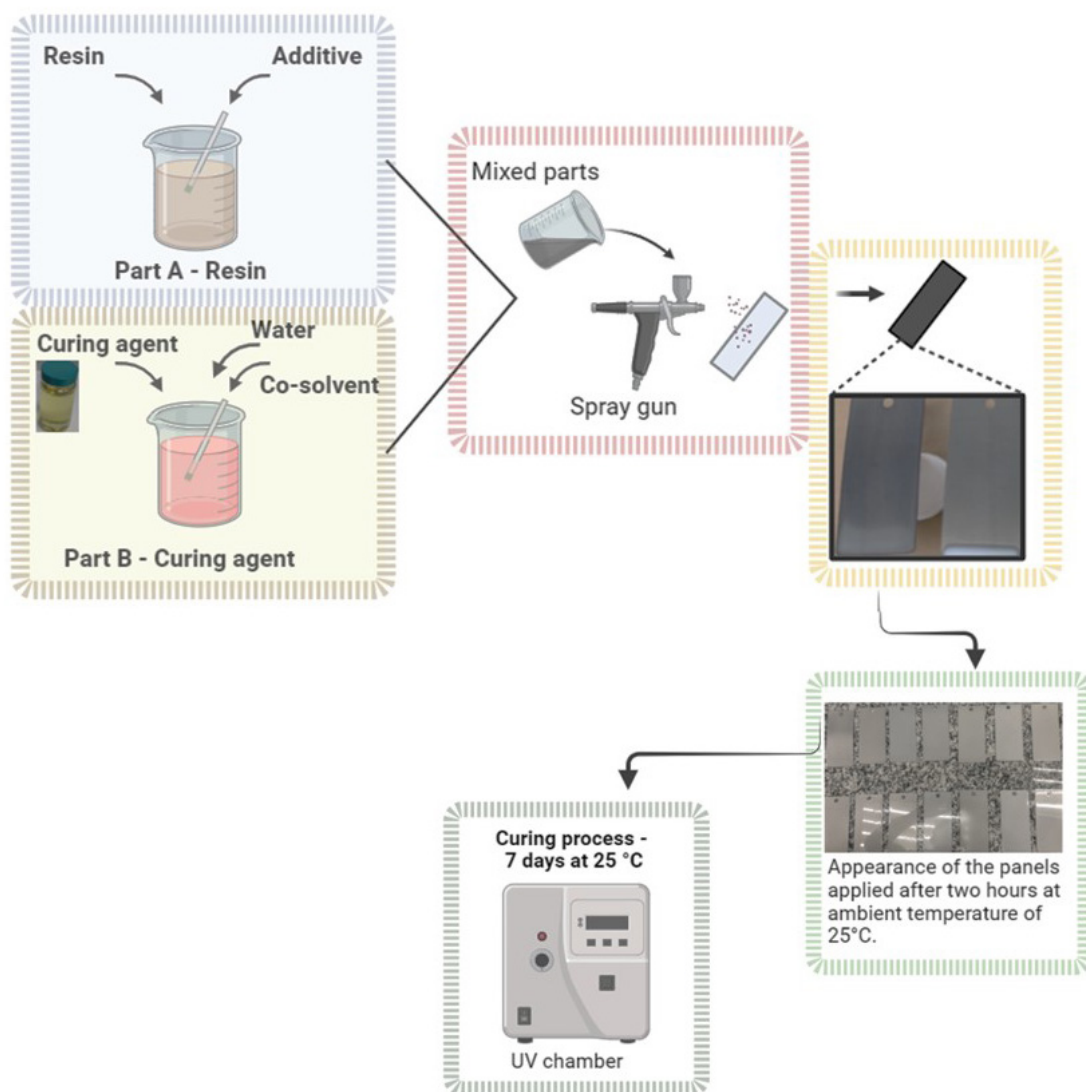


Figure 1. Schematic illustration of the coatings' fabrication technique to produce UV-resistant materials. Created with Biorender.

Table 3. Delta b evolution during the weathering tests at the 7 different times.

Experiment	39 h	109 h	162 h	207 h	375 h	439 h	500 h
1	-0.2	-0.7	1.3	1.7	3.4	3.5	3.5
2	-0.1	-0.1	1.3	1.7	3.2	3.7	3.0
3	1.7	4.1	4.4	4.2	3.4	1.7	-0.05
4	1.1	2.8	3.2	3.4	3.6	0.3	-1.5
5	1.5	1.5	3.6	4.6	7.0	6.8	5.7
6	0.9	4.2	4.1	4.5	-5.5	6.5	4.7
7	1.3	7.3	9.4	-0.6	-4.9	-3.2	-2.9
8	2.0	3.9	-4.3	-3.8	-4.5	-5.1	-6.0
9	3.4	4.3	9.4	6.3	-1.6	-2.2	-1.6
10	2.2	2.8	0.4	-0.8	-7.5	-5.3	-4.7
11	1.8	2.2	2.7	2.8	3.7	4.1	4.1
12	1.9	2.3	2.6	2.6	4.2	5.0	4.7

Instrument Series Q20 (TA Instruments, New Castle, USA). The specimens were heated from -20 °C to 180 °C at a rate of 10 °C/min.

2.3.4 Macroscopic morphology

The coatings' surface morphology was analyzed using a microscope TESCAN VEGA3 from Tescan do Brasil (São Paulo, Brazil). The equipment is equipped with a heated tungsten filament cathode operating at 30 keV. Images were recorded at 500x.

3. Results and Discussions

3.1 Appearance changes - color

Epoxy coatings have a wide range of applications in coatings' field due to their high range of attainable properties and versatility. However, under severe conditions of oxidation, sunlight, and other external agents, the coatings' tend to degrade, resulting in chemical and physical changes. CIELab delta b and delta E parameters during the exposure testing were measured and are presented in Tables 3 and 4. Accelerated weathering usually changes the sample appearance because it changes the reflectance spectra, altering color shade and lightness. Changes in color parameters are usually associated with resin degradation, in this case, the epoxy waterborne resin, by the oxidation and evolution of gaseous and soluble products^[17]. In this case, the aromatic moiety presence absorbs UV radiation, resulting in discoloration and chalking.

The b* parameter is attributed to the yellow-blue axis, and the b* increase in the positive direction indicates the yellowing of coating samples. According to Verma, the overall color difference (ΔE) in PU coatings is best represented by Δb since the epoxy resin absorbs more UV light due to the benzene ring structure^[18]. According to Rivaton et al., the photo-oxidation of epoxy resin involves reactions with the methylene groups in the α -position to the ether groups related to secondary hydroxyl groups dehydration^[19].

In the first weathering hours, experiments 8, 9, and 10 showed the most prominent yellowness (Table 3); these samples were prepared with CU-3 and CU-4, the curing agents with the higher aminic values. After the complete exposure time, it was observed that most experiments

Table 4. T_g results of the investigated coatings before and after aging (0 and 500 h of exposure).

Sample	T _g (°C) Before aging	T _g (°C) After aging	%T _g increase
1	36.2	55.4	+53.0
2	38.4	56.2	+46.4
3	35.3	61.4	+73.9
4	39.5	60.0	+51.9
5	37.9	62.1	+63.9
6	37.2	62.4	+67.7
7	42.0	63.3	+50.7
8	44.3	63.8	+44.0
9	44.6	66.2	+48.4
10	43.5	63.0	+44.8
11	41.0	61.3	+49.5
12	41.9	59.9	+43.0

showed significant color changes over time, and samples with higher b* values for both the negative and positive axis became darker due to oxidation of the degradation products^[20]. According to Ghasemi-Kahrizsangi et al., the color change is associated with light absorption by exciting an electron from the ground state into an excited state by chromophore groups, such as C=C and C=O. After the UV radiation absorption, some discoloration or color change can be observed^[21]. The delta E was evaluated to evaluate the color change in a more detailed way (Table S2 and Figure 2).

Considering the ΔE results, it is observed values between 1 and 16 after 500 h of UV-light exposition. The literature shows a broad range of values that depend on the curing agent and several types of resin. Ghrohrodi et al. prepared epoxy coatings containing nano-porous Zr(IV) and reported ΔE between 5.3 and 7.1. According to the authors, the epoxy coating shows intrinsic low UV resistance (~7), and the use of nanoparticles can decrease the coating damage after UV exposure^[22]. Li et al.^[23] prepared epoxy graphene coatings aiming for weather and corrosion resistance and found ΔE between 4.1 and 15.6. The authors attributed higher delta E values to the absence of graphene, resulting in composites with high sensitivity to color changes, and the smallest values, i.e., most resistant ultraviolet aging samples, were reported as those with 0.5% graphene.

According to DIN 55987^[24,25], the UV stability of coatings is acceptable and highly stable if $\Delta E \leq 2$, but samples that slightly exceed this value can be considered stable if more tests are conducted to confirm the coating performance. In this work, after 20 days of exposure (500 h), only formulation 3 showed acceptable results, followed by 4 and 9, i.e., curing agents CU-2 and CU-4 (both curing agents are unmodified aliphatic amines). The chromophoric groups are expected to react with the curing agents, reducing the chemical groups available to interact with the UV light and decreasing the color changes. On the other hand, samples 6, 7, and 8 showed the strong degradation of the polymeric material, indicating that CU-3 and CU-5 (unmodified aliphatic amine and modified polyamine, respectively) are UV-light unstable and not adequate for the coatings that aim for UV-resistance.

3.2 Appearance changes - gloss

Generally, exposure to weathering results in a marked decrease in gloss due to resin degradation and surface roughness^[11]. Figure 3 shows the gloss 60° evolution at times 0 h and 500 h, and all samples showed a high initial gloss (>90 GU). The gloss values of all coatings, except for sample 8, were almost the same, revealing that the curing agents didn't alter the surface gloss.

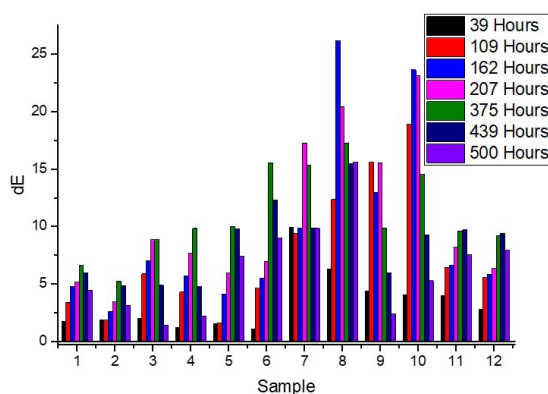


Figure 2. Color variation (delta E) versus samples for each period of weathering.

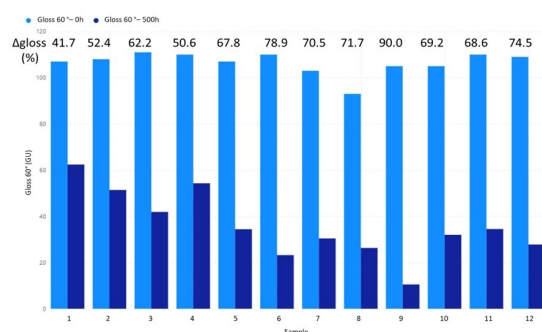


Figure 3. Variations in gloss values measured at times 0 h (light blue columns) and 500 h (dark blue columns) for all the tested samples.

As expected, all samples showed a significant decrease in gloss values associated with photo-degradation after accelerated aging^[12]. According to Rezig et al.^[26], after the photodegradation, the coating surface results in non-homogeneous surfaces with the formation of pits, resulting in an increase in roughness and decrease in thickness, which affects the light reflection and, consequently, gloss values. Another possible reason is that during degradation, organic material loss occurs because of photooxidation, changing the molecular bonds and resulting in microscopic changes in the coatings^[27,28]. Most experiments showed decreases in the gloss higher than 60% after 500 h of weathering, except for samples 1, 2, and 4, suggesting that these samples are more resistant to the weathering conditions than the others. These results agree with the delta E values since the change in surface roughness influences the light interactions with the substrate by decreasing the gloss and affecting the color perception, i.e., high delta E values^[29]. These results are consistent with those presented in SEM results in the next sections.

Samples 1, 2, and 4 were cured with CU-1 and CU-4, and the curing agents have in common the aminic value (between 200 and 300 KOH/g) and the equivalent weight of amine hydrogen (higher than 120 g/eq)^[30]. Besides, according to Klippstein et al.^[13], the curing agent for waterborne formulations can result in incompatibility with the epoxy resin, resulting in several problems, such as the tendency to exude the curing agent to the surface, a decrease of stability, changes in molecular weight and reduced reactivity. In this way, there is a possibility that the CU-3 (unmodified aliphatic amines), CU-4 (unmodified aliphatic amines), and CU-5 (modified polyamine with 55 wt% solids) have a slight incompatibility with the matrix that, at accelerated weathering, reduces the coating resistance. Another fact in agreement with the presented hypothesis is that the amines are more hydrophilic than the epoxy resin, and a possible incompatibility could result in concentrations of amine in localized domains, which, under severe aging conditions, accelerate the film's degradation.

3.3 FTIR

FTIR analysis was conducted to evaluate the chemical structure of the coatings before and after the accelerated weathering (Figure 4). The epoxy resin characteristic peaks include a broad band centered at 3383 cm^{-1} (extra hydroxyl groups generated during the curing reaction), and another between 3018 and 2770 cm^{-1} containing three minor peaks centered at 2973, 2914, and 2868 cm^{-1} , attributed to C-H stretching vibrations from methylene and methyl groups, and C-H bonds of aliphatic and aromatic methine groups^[29]. These peaks were found for all samples after curing.

Other peaks were found at 1740 cm^{-1} (carbonyl groups stretching vibrations), 1605 and 1580 cm^{-1} (C-C stretching of aromatic rings), 1507 cm^{-1} (N-H bending vibrations), 1548 cm^{-1} (stretching vibrations of aromatic rings), 1383, 1359, 1293 cm^{-1} and 1233 cm^{-1} (C-O-C stretch from ether groups), 1180 cm^{-1} (O-H bend), 1106 and 1083 cm^{-1} (C-O vibrations), 939 cm^{-1} (epoxide group C-O-C), 823, 768, and 728 cm^{-1} (C-H out of plane bending), and 552 cm^{-1} (aromatic ring bending)^[22,30-34]. Before the weathering, the samples

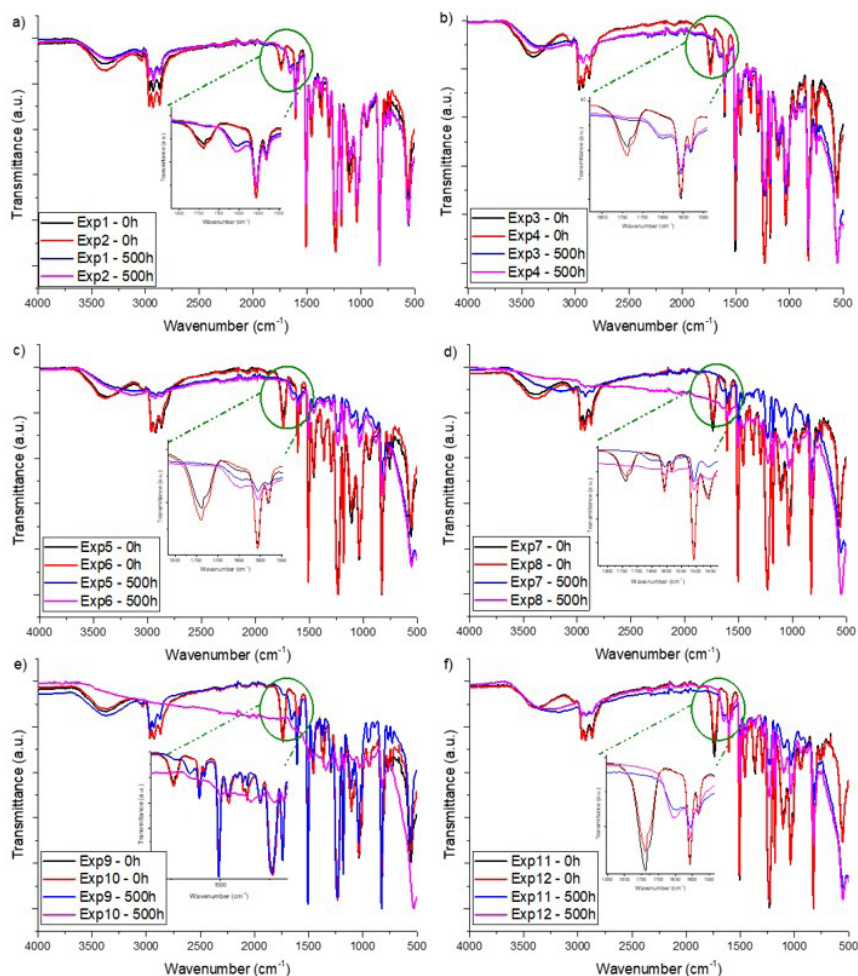


Figure 4. FTIR spectra of samples before (0h) and after (500h) accelerated weathering for the experiments with different curing agents (CU): a) 1 and 2 (CU-1), b) 3 and 4 (CU-2), c) 5 and 6 (CU-5), d) 7 and 8 (CU-1 + CU-3), e) 9 and 10 (CU-1 + CU-4), and f) 11 and 12 (CU-1 + CU-5).

showed very similar FTIR spectra with the main characteristic peaks at the same wavenumber for the different curing agents, as shown in Figure 4.

The curing agent significantly influenced the chemical structure of the films after degradation, highlighting the changes in the region $1800\text{--}1550\text{ cm}^{-1}$, identified in the insert of all the graphs in Figure 4.

The bands in the region $3500\text{--}2900\text{ cm}^{-1}$ showed a decrease in intensity attributed to photooxidation after accelerated aging and the peak located at 1507 cm^{-1} ^[35]. All coatings showed the disappearance of peak 1740 cm^{-1} and a new band at $\sim 1650\text{ cm}^{-1}$ related to aldehyde and peracid formation and the carbonyl formation during oxidation, respectively. The changes in these peaks agree with the photooxidative mechanism proposed by Bellinger and Verdu^[26,36]. During the oxidation process, a ketone formation occurs derived from the secondary OH groups, and amide groups are generated from the abstraction of hydrogen from the methylene groups adjacent to the crosslink.

All the chemical changes are a consequence of epoxy chain scission that results in the formation of carbonyl, hydroperoxide, and other radical groups that are associated with photoreactions. Awad et al. reported that the appearance of carbonyl and hydroxyl groups after degradation results from the oxidation reactions and represents the polymeric scission^[37]. The degradation generally induces surface cracking and loss of mass because of the bioactive transformation products formed during the degradation, which can be released into the environment as gas or leached compounds^[38]. Additionally, after the degradation, the coating becomes more brittle and rigid, increasing the stress absorption and generating microcracks^[39].

Analyzing the FTIR graphs of Figure 4, the chemical structure loss of Experiments 8 and 10 is visible, which is associated with the complete degradation of the samples on a molecular level. Even with different curing agents, it is possible to note that all experiments showed, at least, a slight degradation of the matrix, as highlighted in the Figure 4 inserts, indicating that the coatings maintained a

UV-sensitive characteristic. It is interesting to note that the FTIR data corroborate a degradation of the coating resin in all samples but is more intense for samples 8 and 10, which is coherent with the degradation chemistry since both samples contain unmodified aliphatic amines from the curing agents. This result is related to the large variation in brightness and color observed for these samples, indicating the unfeasibility of using these coatings – and curing agents with aliphatic amines - in applications that require resistance to weathering. According to Bellinger and Verdu, these results can be attributed to the depletion of the oxidizable groups, and the loss of oxidized products formed during the degradation^[36].

3.4 Differential scanning calorimetry

DSC was conducted to evaluate the effect of different curing agents on the coatings' thermal properties by glass transition temperature analysis. The T_g of coatings is mainly influenced by the crosslink density, being a proportional property, i.e., the greater the crosslink density, the higher the T_g ^[37,40]. T_g values of the coatings before and after aging are reported in Table 4. Experiments 7, 8, 9, 10, 11, and 12 showed T_g values higher than 40 °C before the accelerated aging, indicating that the mixture of CU-1 with CU-4 and CU-5 resulted in higher crosslink density when compared

to samples 1-6 that were cured with only one type curing agent, i.e., not a mixture. Samples with high T_g values are expected to have a slower ion diffusion rate and better barrier properties. Besides, the CU mixture probably produces a superior ability to emulsify liquid epoxy resin, resulting in more compact and uniform coatings. Lower T_g values indicate lower free volumes, i.e., less rigid and highly flexible coating.

After the accelerated weathering, all samples showed higher T_g values, which can be associated with the photolysis of the epoxy resin and the QUV temperature that can promote curing reactions or the exudation of some compounds, as previously discussed in FTIR^[28,36]. In this case, if the samples were not completely cured before the test, the completion will occur during the aging, i.e., there are chemical changes. These results indicate that after aging, all samples are harder. According to Xiong and Li, the increase in the T_g values can be a result of dehydration condensation between hydroxide radicals inside the coatings, which can be the key to higher stability^[41].

3.5 Morphology after accelerated weathering

Optical micrographs of the coatings surface of all the samples after the accelerated aging are shown in Figure 5 (400x). The experiments showed different

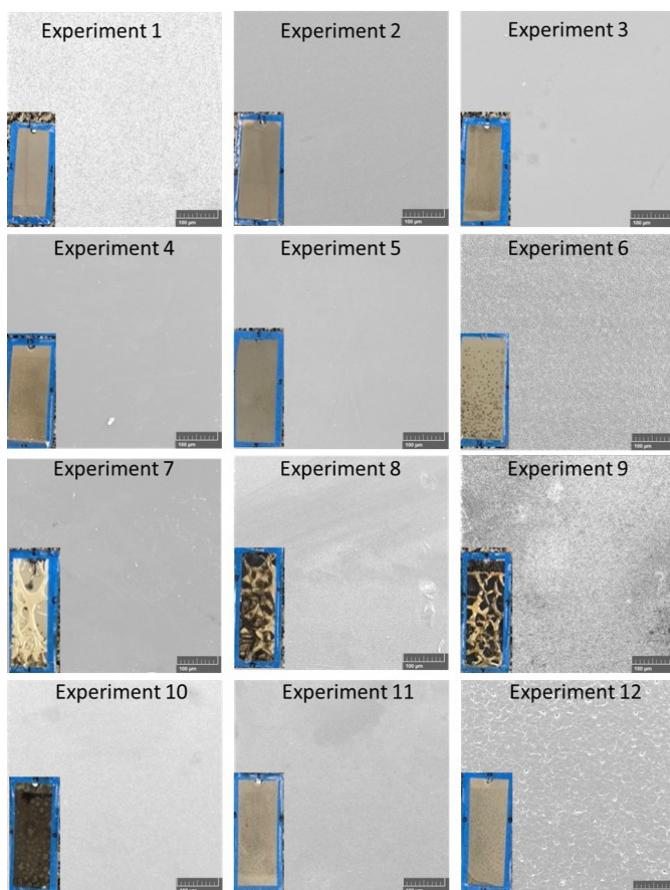


Figure 5. Optical microscopy images of all tested experiments after accelerated weathering (500h of exposure) (500x).

morphological aspects depending on the weathering behavior. Samples 6-10 and 12 showed the worst appearance with a high number of fractures, voids, and a high number of defects. These samples also showed high T_g values, making the coating more rigid and brittle and allowing the materials to absorb stresses. According to Onn et al.^[42], the changes in the surface morphology are associated with blistering, surface segregation, inhomogeneity, and swelling because of polymer network degradation. The observed changes are also associated with surface color change – yellowing, as discussed before, because of chromophoric group generation due to polymer degradation^[9]. Additionally, the gloss reduction is attributed to the high number of protrusions on the surface samples and the increase in light diffusion due to the changes in the microstructures^[4].

Samples 2-5 (one curing agent used), 7 (CU-1+CU-3), 10 (CU-1+CU-4), and 11 (CU-1+CU-5) showed minor visual changes, indicating moderate degradation with fewer weathering products, probably due to the formulations' UV absorption and scattering ability^[30,38,43]. However, macroscopically, samples 7 and 10 showed many defects, which is not possible for future applications. Considering all the results presented in this work, the samples with the best UV-resistance performance are 2 (CU-1), 3 (CU-2), and 4 (CU-2), i.e., the curing agents CU-3 and CU-4 (unmodified aliphatic amines) probably are not adequate for the studied system.

4. Conclusions

This work presented the development and UV-resistance performance of waterborne epoxy coatings with aminic-curable substances. Color and gloss changes, FTIR, thermal properties, and macroscopic morphology evaluated the coatings. Results indicated that samples with higher aminic values tended to degrade faster than those with lower aminic values, as confirmed by higher yellowness and darkness – caused by the oxidation of the polymer and the hydrophilic nature of these groups. Additionally, all samples showed a decrease in gloss values associated with surface roughness and polymer degradation changes. FTIR results confirm the scission of polymer chains with significant changes and the disappearance of the main peaks associated with the epoxy structure. The T_g increased values after weathering might be ascribed to the photo-oxidative products of the coupling reactions due to the photolysis of the resin. The results were confirmed by morphological images that indicated degradation characteristics and loss of structure of some samples and indicated the most suitable samples for future studies and applications. Additionally, comparing the curing agents, those unmodified aliphatic amines showed an inferior performance with a high tendency to degrade under UV environment. Finally, the curing agents with aminic values between 200 and 300 KOH/g and the equivalent weight of amine hydrogen higher than 120 g/eq showed the best performance in epoxy coatings and good stability against accelerated aging, being promising options for future applications.

5. Author's Contribution

- **Conceptualization** – Mauro Sergio da Silva; Ticiane Sanches Valera; Hélio Wiebeck.

- **Data curation** – Mauro Sergio da Silva; Ticiane Sanches Valera; Hélio Wiebeck.
- **Formal analysis** – Mauro Sergio da Silva; Alana Gabrieli de Souza.
- **Funding acquisition** – Derval dos Santos Rosa; Ticiane Sanches Valera; Hélio Wiebeck.
- **Investigation** – Mauro Sergio da Silva; Alana Gabrieli de Souza.
- **Methodology** – Mauro Sergio da Silva; Ticiane Sanches Valera; Hélio Wiebeck.
- **Project administration** – Ticiane Sanches Valera; Hélio Wiebeck.
- **Resources** – Derval dos Santos Rosa; Ticiane Sanches Valera; Hélio Wiebeck.
- **Software** – NA.
- **Supervision** – Derval dos Santos Rosa; Ticiane Sanches Valera; Hélio Wiebeck.
- **Validation** – Mauro Sergio da Silva; Ticiane Sanches Valera; Hélio Wiebeck.
- **Visualization** – Mauro Sergio da Silva; Alana Gabrieli de Souza.
- **Writing – original draft** – Mauro Sergio da Silva; Alana Gabrieli de Souza; Derval dos Santos Rosa; Ticiane Sanches Valera; Hélio Wiebeck.
- **Writing – review & editing** – Mauro Sergio da Silva; Alana Gabrieli de Souza; Derval dos Santos Rosa; Ticiane Sanches Valera; Hélio Wiebeck.

6. Acknowledgements

This research was funded by CNPq (308053/2021-4 and 403934/2021-4) and FAPESP (2022/01382-3, 2021/14714-1, 2020/13703-3). The authors thank the CAPES (Code 001), UFABC, USP, IPT, IPEN, and REVALORES Strategic Unit.

7. References

1. Wang, S., Hu, Z., Shi, J., Chen, G., Zhang, Q., Weng, Z., Wu, K., & Lu, M. (2019). Green synthesis of graphene with the assistance of modified lignin and its application in anticorrosive waterborne epoxy coatings. *Applied Surface Science*, 484, 759-770. <http://doi.org/10.1016/j.apsusc.2019.03.229>.
2. Sheng, X., Li, S., Huang, H., Zhao, Y., Chen, Y., Zhang, L., & Xie, D. (2020). Anticorrosive and UV-blocking waterborne polyurethane composite coating containing novel two-dimensional Ti3C2 MXene nanosheets. *Journal of Materials Science*, 56(6), 4212-4224. <http://doi.org/10.1007/s10853-020-05525-2>.
3. Rashvand, M., Ranjbar, Z., & Rastegar, S. (2011). Nano zinc oxide as a UV-stabilizer for aromatic polyurethane coatings. *Progress in Organic Coatings*, 71(4), 362-368. <http://doi.org/10.1016/j.porgcoat.2011.04.006>.
4. Colonetti, E., Rovani, R., Westrup, J. L., Cercená, R., Carginin, M., Peterson, M., & Dal-Bó, A. G. (2022). Effects of resin/curing agent stoichiometry and coalescence of emulsion particles on the properties of waterborne epoxy coatings upon accelerated weathering. *Materials Chemistry and Physics*, 275, 125228-125238. <http://doi.org/10.1016/j.matchemphys.2021.125228>.
5. Wu, Y., Wu, X., Yang, F., & Ye, J. (2020). Preparation and Characterization of Waterborne UV Lacquer Product Modified

- by Zinc Oxide with Flower Shape. *Polymers*, 12(3), 668-679. <http://doi.org/10.3390/polym12030668>. PMID:32192083.
6. Li, Z., Zhu, L., Xie, X., Zhou, M., Fu, C., & Chen, S. (2023). High-Hardness, Water-Stable, and UV-Resistant Conductive Coatings Based on Waterborne PEDOT:PSS/Epoxy/(KH560/SiO₂) Composite. *Journal of Composites Science*, 7(2), 51-68. <http://doi.org/10.3390/jcs7020051>.
 7. Li, K., Shan, W., Cui, J., Qiu, H., Yand, G., Zheng, S., & Yang, J. (2020). Enhanced corrosion resistance and weathering resistance of waterborne epoxy coatings with polyetheramine-functionalized graphene oxide. *Journal of Coatings Technology and Research*, 17(1), 171-180. <http://doi.org/10.1007/s11998-019-00252-z>.
 8. Liu, F., Zheng, M., Fan, X., Li, H., & Wang, F. (2021). Performance evaluation of waterborne epoxy resin-SBR compound modified emulsified asphalt micro-surfacing. *Construction & Building Materials*, 295, 123588. <http://doi.org/10.1016/j.conbuildmat.2021.123588>.
 9. Nikafshar, S., McCracken, J., Dunne, K., & Nejad, M. (2021). Improving UV-stability of epoxy coating using encapsulated halloysite nanotubes with organic UV-stabilizers and lignin. *Progress in Organic Coatings*, 151, 105843. <http://doi.org/10.1016/j.porgcoat.2020.105843>.
 10. Woo, R. S. C., Chen, Y., Zhu, H., Li, J., Kim, J.-K., & Leung, C. K. Y. (2007). Environmental degradation of epoxy-organoclay nanocomposites due to UV exposure. Part I: photo-degradation. *Composites Science and Technology*, 67(15-16), 3448-3456. <http://doi.org/10.1016/j.compscitech.2007.03.004>.
 11. Huo, S., Liu, Z., Li, C., Wang, X., Cai, H., & Wang, J. (2019). Synthesis of a phosphaphenanthrene/benzimidazole-based curing agent and its application in flame-retardant epoxy resin. *Polymer Degradation & Stability*, 163, 100-109. <http://doi.org/10.1016/j.polymdegradstab.2019.03.003>.
 12. Wang, C., Huo, S., Ye, G., Song, P., Wang, H., & Liu, Z. (2023). A P/Si-containing polyethylenimine curing agent towards transparent, durable fire-safe, mechanically-robust and tough epoxy resins. *Chemical Engineering Journal*, 451(Part 2), 138768-138771. <http://doi.org/10.1016/j.cej.2022.138768>.
 13. Klippstein, A., Cook, M., & Monaghan, S. (2012). *Water-based epoxy systems*. In K. Matyjaszewski, & M. Möller (Eds.), *Polymer science: a comprehensive reference* (pp. 519-539), Netherlands: Elsevier. <http://doi.org/10.1016/B978-0-444-53349-4.00281-8>.
 14. Asada, C., Honjo, K., & Nakamura, Y. (2021). Utilization of steam-treated and milling-treated lignin from moso bamboo as curing agent of epoxy resin. *Waste and Biomass Valorization*, 12(11), 6261-6272. <http://doi.org/10.1007/s12649-021-01444-8>.
 15. American Society for Testing and Materials – ASTM. (2023). *ASTM G154-23 -Standard Practice for Operating Fluorescent Ultraviolet (UV) Lamp Apparatus for Exposure of Materials*. USA: ASTM International.
 16. Yari, H., & Rostami, M. (2020). Enhanced weathering performance of epoxy/ZnO nanocomposite coatings via functionalization of ZnO UV blockers with amino and glycidoxy silane coupling agents. *Progress in Organic Coatings*, 147, 105773. <http://doi.org/10.1016/j.porgcoat.2020.105773>.
 17. Yang, X. F., Tallman, D. E., Bierwagen, G. P., Croll, S. G., & Rohlik, S. (2002). Blistering and degradation of polyurethane coatings under different accelerated weathering tests. *Polymer Degradation & Stability*, 77(1), 103-109. [http://doi.org/10.1016/S0141-3910\(02\)00085-X](http://doi.org/10.1016/S0141-3910(02)00085-X).
 18. Verma, G. (2019). Weathering, salt spray corrosion and mar resistance mechanism of clay (nano-platelet) reinforced polyurethane nanocomposite coatings. *Progress in Organic Coatings*, 129, 260-270. <http://doi.org/10.1016/j.porgcoat.2019.01.028>.
 19. Rivaton, A., Moreau, L., & Gardette, J.-L. (1997). Photo-oxidation of phenoxy resins at long and short wavelengths: II. Mechanisms of formation of photoproducts. *Polymer Degradation & Stability*, 58(3), 333-339. [http://doi.org/10.1016/S0141-3910\(97\)00088-8](http://doi.org/10.1016/S0141-3910(97)00088-8).
 20. Herrera, R., Muszynska, M., Krystofiak, T., & Labidi, J. (2015). Comparative evaluation of different thermally modified wood samples finishing with UV-curable and waterborne coatings. *Applied Surface Science*, 357(Pt B), 1444-1453. <http://doi.org/10.1016/j.apsusc.2015.09.259>.
 21. Ghasemi-Kahrizsangi, A., Neshati, J., Shariatpanahi, H., & Akbarinezhad, E. (2015). Improving the UV degradation resistance of epoxy coatings using modified carbon black nanoparticles. *Progress in Organic Coatings*, 85, 199-207. <http://doi.org/10.1016/j.porgcoat.2015.04.011>.
 22. Ghohrodi, A. R., Ramezanzadeh, M., & Ramezanzadeh, B. (2022). Investigating the thermo-mechanical and UV-shielding properties of a nano-porous Zr(IV)-type metal-organic framework (MOF) incorporated epoxy composite coating. *Progress in Organic Coatings*, 164, 106693. <http://doi.org/10.1016/j.porgcoat.2021.106693>.
 23. Li, Z.-J., Wang, F.-S., Lai, Y.-C., Shi, Z.-E., & Yu, Y.-H. (2021). Flexible epoxy graphene thermoset with excellent weather and corrosion resistance. *Progress in Organic Coatings*, 151, 106052. <http://doi.org/10.1016/j.porgcoat.2020.106052>.
 24. Zeng, W., Zhou, Q., Zhang, H., & Qi, X. (2018). One-coat epoxy coating development for the improvement of UV stability by DPP pigments. *Dyes and Pigments*, 151, 157-164. <http://doi.org/10.1016/j.dyepig.2017.12.058>.
 25. Erzožnik, H., Razboršek, T., & Gunde, M. K. (2016). Characterization of orange pigments in decorative outdoor coatings and their weather fastness. *Progress in Organic Coatings*, 99, 47-54. <http://doi.org/10.1016/j.porgcoat.2016.05.007>.
 26. Rezig, A., Nguyen, T., Martin, D., Sung, L., Gu, X., Jasmin, J., & Martin, J. W. (2006). Relationship between chemical degradation and thickness loss of an amine-cured epoxy coating exposed to different UV environments. *Journal of Coatings Technology and Research*, 3(3), 173-184. <http://doi.org/10.1007/BF02774507>.
 27. Bano, H., Khan, M. I., & Kazmi, S. A. (2011). Structure and microstructure studies of epoxy coating after natural exposure testing. *Journal of the Chemical Society of Pakistan*, 33(4), 454-463. Retrieved in 2024, March 25, from <https://jcsp.org.pk/ArticleUpload/3126-14641-1-PB.pdf>
 28. Yang, J.-W., Cho, H.-J., & Gong, Y.-D. (2023). Analytical approach to degradation structural changes of epoxy-dicyandiamide powder coating by accelerated weathering. *Progress in Organic Coatings*, 175, 107357. <http://doi.org/10.1016/j.porgcoat.2022.107357>.
 29. Amrollahi, S., Yari, H., & Rostami, M. (2022). Investigating the weathering performance of epoxy silicone nanocomposite coatings containing various loadings of Glycidoxypropyltrimethoxysilane-modified Zinc oxide nanoparticles. *Progress in Organic Coatings*, 172, 107094. <http://doi.org/10.1016/j.porgcoat.2022.107094>.
 30. Wang, J., Ma, L., Ding, X., Xu, H., Wang, Y., Zhao, M., Ren, C., & Zhang, D. (2023). Tea polyphenol radical scavenger loaded UV absorber for corrosion resistant and weathering resistant epoxy coating fabrication. *Progress in Organic Coatings*, 180, 107553. <http://doi.org/10.1016/j.porgcoat.2023.107553>.
 31. Soleimani, M., Bagheri, E., Mosaddegh, P., Rabiee, T., Fakhari, A., & Sadeghi, M. (2021). Stable waterborne epoxy emulsions and the effect of silica nanoparticles on their coatings properties. *Progress in Organic Coatings*, 156, 106250. <http://doi.org/10.1016/j.porgcoat.2021.106250>.
 32. Li, R., Leng, Z., Zhang, Y., & Ma, X. (2019). Preparation and characterization of waterborne epoxy modified bitumen

- emulsion as a potential high-performance cold binder. *Journal of Cleaner Production*, 235, 1265-1275. <http://doi.org/10.1016/j.jclepro.2019.06.267>.
33. Udoh, I. I., Shi, H., Liu, F., & Han, E.-H. (2020). Microcontainer-based waterborne epoxy coatings for AA2024-T3: effect of nature and number of polyelectrolyte multilayers on active protection performance. *Materials Chemistry and Physics*, 241, 122404. <http://doi.org/10.1016/j.matchemphys.2019.122404>.
 34. Wörnheim, A., Edvinsson, C., Sundell, P.-E., Heydari, G., Deltin, T., & Persson, D. (2022). Depth-resolved FTIR-ATR imaging studies of coating degradation during accelerated and natural weathering: influence of biobased reactive diluents in polyester melamine coil coating. *ACS Omega*, 7(27), 23842-23850. <http://doi.org/10.1021/acsomega.2c02523>. PMID:35847300.
 35. Bellinger, V., Bouchard, C., Claveirolle, P., & Verdu, J. (1981). Photooxidation of epoxy resins cured by non-aromatic amines. *Photochemistry*, 1(1), 69-80. [http://doi.org/10.1016/0144-2880\(81\)90016-6](http://doi.org/10.1016/0144-2880(81)90016-6).
 36. Bellinger, V., & Verdu, J. (1985). Oxidative skeleton breaking in epoxy amine networks. *Journal of Applied Polymer Science*, 30(1), 363-374. <http://doi.org/10.1002/app.1985.070300132>.
 37. Awad, S. A., Mahini, S. S., & Fellows, C. M. (2019). Modification of the resistance of two epoxy resins to accelerated weathering using calcium sulfate as a photostabilizer. *Journal of Macromolecular Science – Part A*, 56(4), 316-326. <http://doi.org/10.1080/10601325.2019.1578179>.
 38. Bell, A. M., Keltsch, N., Shweyen, P., Reifferscheid, G., Ternes, T., & Buchinger, S. (2021). UV aged epoxy coatings—Ecotoxicological effects and released compounds. *Water Research X*, 12, 100105. <http://doi.org/10.1016/j.wroa.2021.100105>. PMID:34189451.
 39. Fernández-Álvarez, M., Velasco, F., & Bautista, A. (2021). Performance of ultraviolet exposed epoxy powder coatings functionalized with silica by hot mixing. *Journal of Materials Research and Technology*, 10, 1042-1057. <http://doi.org/10.1016/j.jmrt.2020.12.094>.
 40. Levin, J. R., Daisey, G., Elbert, K. C., Mallardi, J., Westmeyer, M., & Williams, D. (2023). *Acrylic binder and formulation design for more sustainable Elastomeric Cool Roof Coatings (ERCs)*. In H. N. Cheng, & R. A. Gross (Eds.), *Sustainable green chemistry in polymer research* (Vol. 2, pp. 203-218). USA: American Chemical Society.
 41. Xiong, A., & Li, J. (2023). Constructing stable transparent hydrophobic POSS@epoxy-group coatings for waterproofing protection of decorative-painting surfaces. *Polymer Bulletin*, 81(2), 1403-1419. <http://doi.org/10.1007/s00289-023-04780-y>.
 42. Onn, M., Ahmad, Z., Zainuddin, A., & Iliyas, S. M. M. (2022). Morphology and characterization study on effective microorganism (EM) water based epoxy coatings. *Materials Today: Proceedings*, 66(Pt 10), 4026-4032. <http://doi.org/10.1016/j.matpr.2022.05.334>.
 43. Gao, T., He, Z., Hihara, L. H., Mehr, H. S., & Soucek, M. D. (2019). Outdoor exposure and accelerated weathering of polyurethane/polysiloxane hybrid coatings. *Progress in Organic Coatings*, 130, 44-57. <http://doi.org/10.1016/j.porgcoat.2019.01.046>.

Received: Mar. 25, 2024

Revised: June 18, 2024

Accepted: June 24, 2024

Supplementary Material

Supplementary material accompanies this paper.

Table S1. Characteristics of the catalysts (curing agents) and the main differences considering their properties.

Table S2. Delta E evolution during the weathering tests at the 7 different times.

This material is available as part of the online article from <https://doi.org/10.1590/0104-1428.20230133>